Theoretical Analysis to Determine the Solar Concentration Limit with Passive Cooling of Solar Cells

Ashwin Date*[1], Abhijit Date [1], Aliakbar Akbarzadeh [1]

*[1]RMIT University, School of Aerospace, Mechanical and Manufacturing Engineering, Energy CARE Group, Bundoora East Campus, Melbourne, Australia

*[1]ashwinshridhar.date@rmit.edu.au

Abstract

This research was conducted to determine the limiting values of the geometric concentration when used with solar thermal system (thermoelectric generator) (TEG) to maintain desired hot and cold side temperatures for power generation. An optimum heat sink fin gap is considered to achieve maximum heat transfer rate using passive cooling. A theoretical model is developed for determining the optimum solar concentration using a thermoelectric generator sandwiched between the target plate and passive cooling heat sink. Thermal resistance and Seebeck coefficient of a thermoelectric generator under consideration is experimentally determined. Heat flow path for this system is defined and energy balance equations are established. A computer model is developed to solve the energy balance equations and find the optimum values for geometric concentration and hot & cold side temperature of thermoelectric generator. It was observed that for the specific configuration of heat sink and thermoelectric generator in a system, the trend of temperature difference between the hot and cold sides remain the same at different heat input conditions. The optimum geometric concentration for solar radiation intensity of 800 W/m2 and heat sink fin length of 0.15m is predicted to be 13. The theoretical model is capable of optimizing the values of geometric concentration for desired hot side or cold side temperature.

Keywords

Heat Sink Cooling; Passive Cooling; Solar Concentration; Thermoelectric Generator

Introduction

In last few decades solar energy has shown a great potential in replacing the use of fossil fuel in producing electrical energy. Most of the research is concentrated on developing new technologies for conversion of energy from sun to electricity, and improving the performance of existing technologies. Concentrated solar systems are being widely studies in recent times, and have shown a great potential in improving the performance of existing systems as well as makes the design more compact. One of the technologies used with concentrated solar systems involve the use of thermoelectric generator (TEG) for conversion of the thermal energy from the solar concentrator to area from solar concentrator system can be used as a source of hot side for the TEG, and the other side of TEG is maintained at lower temperature to generate electricity. Maintaining the other side of TEG at lower temperature requires cooling.

Cooling of solar cells has been a topic of great concern for the renewable energy society around the world since last few decades. Much work has been done in developing the new techniques for cooling of solar cells. Most of these techniques involve the use of active systems to extract the heat from the source and transfer it away to the sink. Use of active cooling systems involves some mechanisms that consists moving parts such as fan. Considering the performance characteristics of TEG available in the market commercially, we cannot afford to have an auxiliary power input to such system that would reduce the net power output. To deal with this issue many passive cooling techniques have been designed and presented by researchers in the past [1-4]. Heat sink with fins is most widely preferred passive cooling technique that uses increased surface area for enhancing the heat transfer. This paper focuses on optimizing the design of a solar concentrated system with heat sink cooling of TEG (passive cooling system). A computer model is developed to determine the limits of the solar concentration to maintain the definite temperature difference across the hot and cold side of TEG. The computer program gives us flexibility of varying the input parameters while optimizing the output parameters for defined constraints.electricity.

TEG works on the principle of Seebeck effect where two junctions of dissimilar metals are maintained at different temperatures that give rise to flow of current through those metals. The high temperature target

Heat Flow Path

Incident solar radiations coming from the sun are optically concentrated using the Fresnel lens. The characteristics of square Fresnel lens manufactured from plastic having approximate thickness of 4mm were considered for design of a theoretical model. Optically concentrated solar radiations are directed to fall on the target area below the lens. The Geometric concentration at target could be determined simply by taking the ratio of the aperture area and the target area. Target area has a plate of the desired target area manufactured from high conductivity material. As shown in figure 1 Fresnel lens concentrates the incident solar radiation at the target plate. Thermoelectric generator is sandwiched between the target plate and the heat sink as shown in Figure 1.

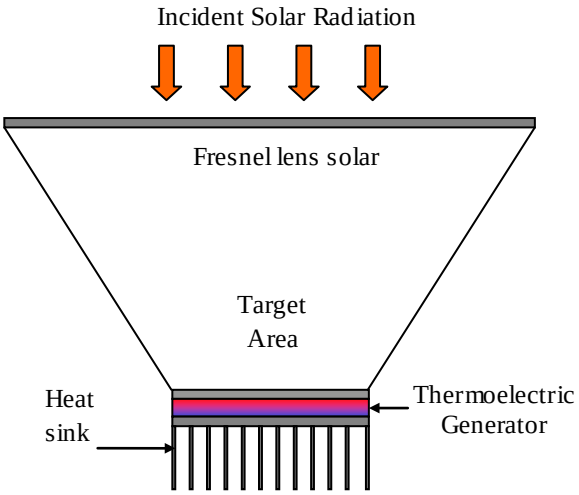

FIG. 1 SOLAR CONCENTRATION SYSTEM

The whole system shown in Figure 1 is further divided into 3 parts for the ease of heat transfer analysis. Figure 2 illustrates the Fresnel lens that is used for concentrating solar radiation and achieves the high-density heat flux at focal area. Incoming solar radiation (I) would fall on the Fresnel lens with an aperture area of (Ap). Aperture area of Fresnel lens will decide the total heat incident on the target area can be adjusted by varying the distance of target area from the aperture. Transmission losses in the Fresnel lens are dependent on the physical parameters of the Fresnel lens. Some of the solar radiation incident on Fresnel lens will get reflected back depending on the reflectivity of the lens. Some of the solar radiation will be refracted away from the target depending on the refractive index of the material of the lens. Manufacturing faults can also lead to some inefficiency in the Fresnel lens. Optical efficiency of the Fresnel lens is assumed to be 60% for this simulation[1, 2].area. This paper considers a square Fresnel lens that has a point focus. Geometrical concentration on the target

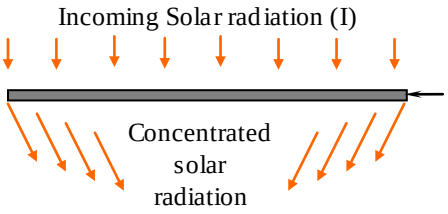

FIG. 2 POINT FOCUS FRESNEL LENS

The concentrated solar radiation hits the aluminum target plate. Schematic of target plate and the thermoelectric generators are illustrated in Figure 3. Thermoelectric generators are attached at the back surface of the target plate. Thermal paste is used between the thermoelectric generator surface and target surface to minimize the contact thermal resistance. Target plate is painted black to absorb most of the incident concentrated solar radiation. As the temperature of the target plate increases, its top exposed surface loses some heat due to radiation heat transfer loss as well as convective heat transfer loss to the ambient air. Rest of the heat is conducted through the thickness of the high conductive target plate. Target plate is assumed to be in isothermal state for the further theoretical analysis.

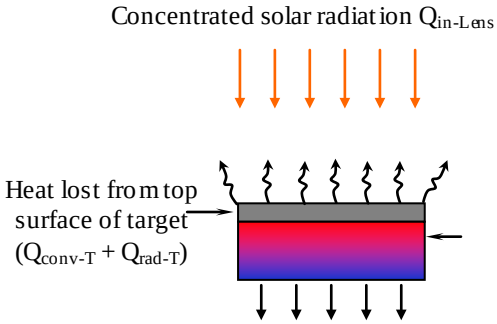

FIG. 3 SCHEMATIC OF HEAT DISTRIBUTION BETWEEN TARGET AREA AND THERMOELECTRIC GENERATOR

Figure 3 illustrates the schematic of heat distribution across target area and thermoelectric generators. The amount of heat lost to the ambient in form of radiation and convection from the top surface of the target plate is stated as Qconv-T and Qrad-T. Radiation and convection losses from this surface are determined

based on the estimation of the convective heat transfer coefficient, emissivity of the top surface and assuming some ambient temperature. Remaining heat is transferred through the thermoelectric generator. Depending on the thermal resistance of thermoelectric generator we can determine the heat transfer through it.

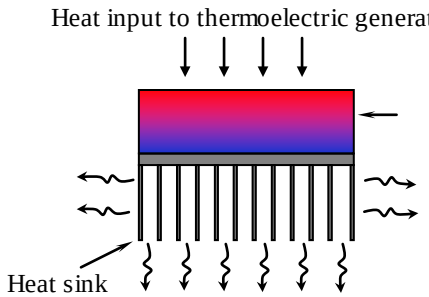

FIG. 4 SCHEMATIC OF HEAT DISTRIBUTION BETWEEN THERMOELECTRIC GENERATORS AND HEAT SINK

Figure 4 illustrates the schematic for the heat flow path across the thermoelectric generators and heat sink to dissipate the heat. As a result of concentrated solar radiation on the target surface, its temperature increases rapidly. The top surface of thermometric generator is in contact with the target area that is at high temperature, and transfers some heat through it as mentioned earlier. The heat at the other end of thermoelectric generator must be dissipated to maintain its temperature to lower values. As shown in Figure 4, heat sink is attached at the bottom surface of the thermoelectric generators that is used to enhance the heat transfer rate at from bottom surface. The energy balance equations for the heat flows mentioned in the Figure 3 and 4 are presented in theoretical analysis section.

Experimental Estimation of Thermal Resistance for TEG

An experimental rig was setup to determine the thermal resistance and the Seebeck coefficient of the available thermoelectric generator. Obtained experimental results will further be used as input values to the simulation. As shown in Figure 5 experimental setup consists of an insulated TEG test rig, variable AC power supply, electronic load and a temperature data logger.

A variable electronic load is used to maintain the power output of TEG at its peak. Temperature is measured at key positions using J type thermocouples connected to the data logger. Variable AC power supply is connected to the electric heater such that we can vary the power supplied and the TEG hot side temperature.

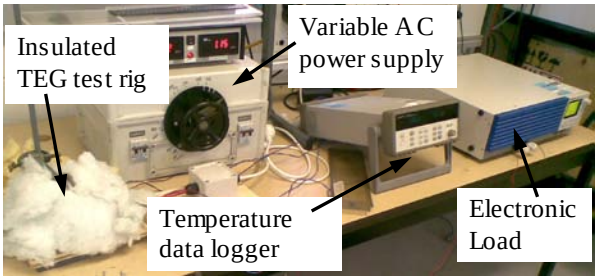

FIG. 5 EXPERIMENTAL SETUP TO DETERMINE THE THERMAL RESISTANCE AND SEEBECK COEFFICIENT OF TEG

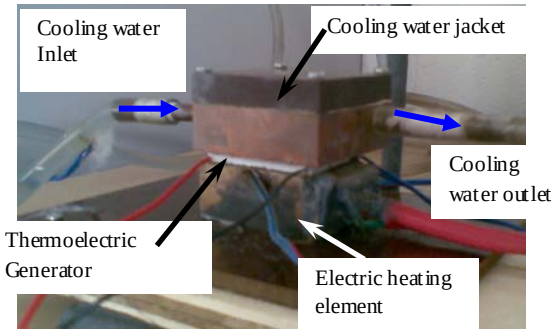

FIG. 6 INSIDE INSULATED TEG TEST RIG

As shown in Figure 6 the insulated TEG test rig consists of an electric heating element that can be supplied with regulated AC power supply, a thermoelectric generator, and a water-cooling jacket. Thermoelectric generator is sandwiched between the electric heater and the water cooling jacket. While performing the experiment this rig is insulated using the glass wool to minimize the heat losses. Still small amount of heat is lost in convection and radiation and rest flows through the thermoelectric generator. Thermoelectric generator offers the thermal resistance to the flow of heat. At different heat inputs the temperatures of hot and cold side of TEG as well as the cooling water inlet and cooling water outlet temperature is recorded. The heat balance equation is formulated to determine the thermal resistance offered by the TEG. The plot for thermal resistance of the TEG used for this experiment is illustrated in Figure 7.

It is observed that the TEG offers the thermal resistance of in the range of 0.88°C/W to 1.05°C/W when tested for hot side temperature between 60°C and 150°C. Open circuit voltage and temperatures of hot and cold side of TEG are recorded to determine the Seebeck coefficient of the TEG. The Seebeck coefficient of 0.0527 V/°C was determined for the same temperature range. Average thermal resistance of thermoelectric generator will be assumed to be

0.95 °C/W and average Seebeck coefficient of 0.0527 V/°C will be considered for all the further calculations and computer simulation.

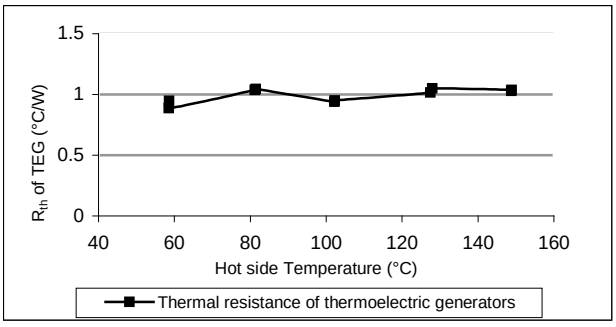

FIG. 7 THERMAL RESISTANCE OFFERED BY THE THERMOELECTRIC GENERATORS AT DIFFERENT TEG HOT SIDE TEMPERATURES

Theoretical Analysis

The thermoelectric generator is sandwiched between the target plate as a heater and the heat sink as a cooling device to achieve the temperature difference across TEG. Optical efficiency of Fresnel lens is considered to be 60%. Total heat input to the system could be determined depending on the aperture area of the concentrator lens. Thermal analysis of the total system is presented in two sections. The total amount of heat coming in from the lens aperture area is given by

$$Q_{In-lens} = Q_{In1} = I \times A_p \times \eta_{opt} \qquad (1)$$

I is the average incident solar heat flux on the surface of the lens. Average incident solar heat flux on the earth surface would vary with the latitude and time of the year under consideration. For this analysis we have assumed it to be 800W/m^2.

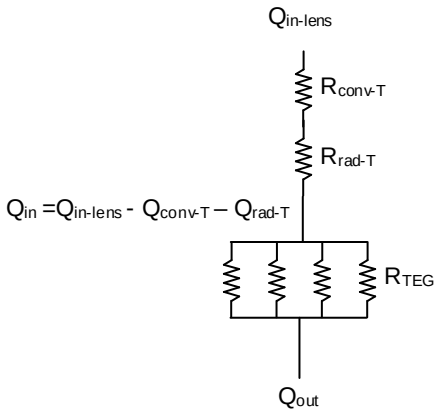

FIG. 8 THERMAL RESISTIVE CIRCUIT FOR HEAT FLOW THROUGH TARGET PLATE AND THERMOELECTRIC GENERATORS

Figure 8 demonstrates the thermal resistive circuit for the heat distribution between target area and thermoelectric generators. Thermoelectric generators offer a thermal resistance for the flow of heat. Rconv-T and Rrad-T in the circuit diagram are the thermal resistances offered by the convective and radiation losses from the top surface of target area. RTEG in the circuit diagram represents the thermal resistance offered by the thermoelectric generators. Thermal resistance is determined experimentally and explained in detail in the earlier section. Convection heat transfer loss from the top surface of target area is given by

$$Q_{conv-T} = h_t \times A_t \times (T_s - T_a) \qquad (2)$$

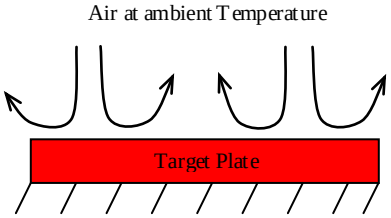

FIG. 9 NATURAL CONVECTION COOLING FOR HORIZONTAL HOT SURFACE FACING UPWARD DIRECTION

h_t represents the convective heat transfer coefficient of the target surface. Target plate is assumed to be isothermal horizontal surface with hot side facing in upward direction. Extensive research has previously been done to determine the Nusselt number for the above mentioned condition[3, 4].

$$N_u = 0.54(G_r P_r)^{1/4} \qquad 10^4 <= N_u <= 10^7 \qquad (3)$$

Emissivity (ε) for aluminium target plate is assumed to be 0.95.The radiation heat transfer loss from the target area is given by

$$Q_{rad-T} = \sigma \times \varepsilon \times A_t \times (T_s^4 - T_a^4) \qquad (4)$$

Heat flow through the thermoelectric generator is given by

$$Q_{TEG} = \frac{1}{R_{TEG}} \times A_{TEG} \times (T_s - T_c) \qquad (5)$$

TEG surface area is considered to be equal to the target area. The total energy balance equation (for the first section as shown in Figure 8) consisting of the target plate and the TEG and can be determined by equating the total heat reaching the target plate (Qin) and the total heat that is transferred through TEG

$$Q_{in-Lens} - Q_{conv-T} - Q_{rad-T} = Q_{TEG} \quad (6)$$

$$\begin{pmatrix} I \times A_p \times \eta_{opt} \\ -h_t \times A_t \times (T_s - T_{amb}) \\ -\sigma \times \varepsilon \times A_t \times (T_s^4 - T_{amb}^4) \end{pmatrix} = \left(\frac{1}{R_{TEG}} \times A_t \times (T_s - T_c) \right) \quad (7)$$

This energy balance equation has two unknown terms of temperature of target plate (Ts), which is also equal to the hot side temperature of the TEG and cold side temperature (Tc). By expanding and rearranging equation 7 we can determine the term for cold side temperature.

$$T_c = \frac{1}{A_t} \begin{pmatrix} A_t T_s - R_{th} I A_p \eta_{opt} \\ -A_t \left[R_{th} \sigma \varepsilon T_s^4 + R_{th} \sigma \varepsilon T_a^4 \right] \\ -h_t A_t \left[R_{th} T_s - R_{th} T_a \right] \end{pmatrix} \quad (8)$$

Second section of the thermal analysis consists of the TEG and the passive cooling heat sink. Thermal resistive circuit for heat flow through thermoelectric generator and heat sink is illustrates in Figure 9.

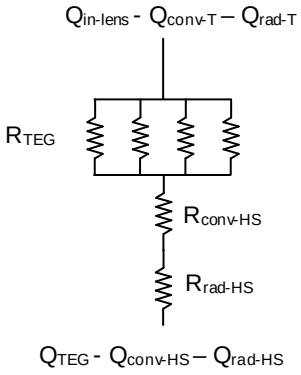

FIG. 10 THERMAL RESISTIVE CIRCUIT FOR HEAT FLOW THROUGH THERMOELECTRIC GENERATORS AND HEAT SINK

Heat passed through the thermoelectric generator depends upon the thermal resistance offered by it. The value of heat passing through the thermoelectric generator will determine the cold side temperature. Efficiency of thermoelectric generator is limited by the Carnot efficiency for the available temperature difference across the hot and cold side. This promotes to have the device that can dissipate the available heat at the cold side of the thermoelectric generator to increase the electrical power output from the thermoelectric generator. Heat sink passive cooling is used in this analysis. Energy balance can be formulated for the second section by equating heat input with heat output from the system. Where heat output from the system is determined by sum of heat transferred through thermoelectric generator (QTEG) and heat lost by radiation heat transfer and convection heat transfer from heat sink (Qrad-hs, Qconv-hs).

Heat sink is attached to the bottom surface of the thermoelectric generator. From the findings of Zhang [5] it is clear that maintaining optimum spacing between the heat sink fins is important to achieve the maximum heat transfer rate. Optimum fin spacing for maximum heat transfer is considered for this analysis.

$$D_{opt} = \frac{4}{3}\delta \quad (9)$$

δ is the boundary layer thickness of natural convection air along the length of the fin. The optimum fins spacing will determine the total number of fins that can fit on the heat sink. And total number of fins will influence the surface area of heat sink (Ahs) available for convection and radiation heat transfer. Convection heat transfer from the heat sink is given by

$$Q_{conv-T} = h_{hs} \times A_{hs} \times (T_c - T_a) \quad (10)$$

Convective heat transfer coefficient for heat sink fin is determined by using the Nusselt number relation for natural convection over vertical surfaces[6].

$$N_u = 0.10 (G_r P_r)^{1/3} \qquad 10^9 <= N_u <= 10^{11} \quad (11)$$

The radiation heat losses at the target area are given by

$$Q_{rad-hs} = \sigma \times \varepsilon \times A_{hs} \times (T_c^4 - T_a^4) \quad (12)$$

Using Equation 5, 10 and 11 we can obtain energy balance equation for second section of the system shown as shown in Figure 9.

$$Q_{TEG} = Q_{conv-hs} + Q_{rad-hs} \quad (13)$$

$$\frac{1}{R_{th}} \times A_t \times (T_s - T_c) = \begin{pmatrix} h_{hs} \times A_{hs} \times (T_c - T_a) \\ +\sigma \times \varepsilon \times A_{hs} \times (T_c^4 - T_a^4) \end{pmatrix} \quad (14)$$

Heat balance equation for second section also has similar two unknown temperature terms as in the heat balance equation for first section. By rearranging and second heat balance equation, we can again find another equation for cold side temperature of thermoelectric generator (Tc).

$$T_c = \frac{1}{A_t} \begin{pmatrix} A_t T_s - \\ h_{hs} A_{hs} \left[R_{th} T_c - R_{th} T_a \right] - \\ A_{hs} \left[R_{th} \sigma \varepsilon T_c^4 - R_{th} \sigma \varepsilon T_a^4 \right] \end{pmatrix} \quad (15)$$

Both the energy equations are solved simultaneously by using the non-linear equation solver in Microsoft

excel program. The solver function from the Microsoft Excel program uses the generalized reduced gradient algorithm to iterate and solve the non-liner equations and find the optimum solutions for the unknown terms in the equations.

A generalised equation for power generation of TEG is used to estimate the electrical power output from the simulated results.

$$P_{TEG} = I_{sc}(T_s - T_c)\alpha - I_{sc}^2 R \quad (16)$$

With the knowledge of hot side and cold side temperature of TEG and using the experimentally determined values of Seebeck coefficient (α), Short circuit current and internal resistance offered by TEG, we could estimate the electrical power generation by the TEG.

Discussion

The concentrated solar thermal system considered in this research has few parameters that need constraint depending upon the variation of thermoelectric generator considered in the system. Fixed parameter in this simulation will be ambient temperature, thermal resistance of TEG, optical efficiency of Fresnel lens and heat sink fin length. The temperature of the hot and cold side of thermoelectric generator for certain geometric concentration ratio can be predicted using the computer simulation. Simulation was performed for different variation of the input parameters and their effects on the output parameters were studied. Simulation results for various conditions were predicted by varying the input conditions such as aperture area, geometric concentration. For the first computer simulation following input conditions was considered.

TABLE 1 INPUT PARAMETERS FOR FIRST SIMULATION

Parameters	**Value (Unit)**
Aperture Area (A_p)	1 m^2
Incident Solar Radiation Intensity (I)	800 W/m^2
Optical Efficiency of solar concentrator (η_{opt})	0.6
Ambient Temperature (T_a)	298 K
Thermal resistance of TEC (R_{th})	0.95 $°C/W$

By keeping all the input parameters to be constant and varying the geometric concentration computer model was used to predict the values for hot and cold side temperature variation of thermoelectric generator.

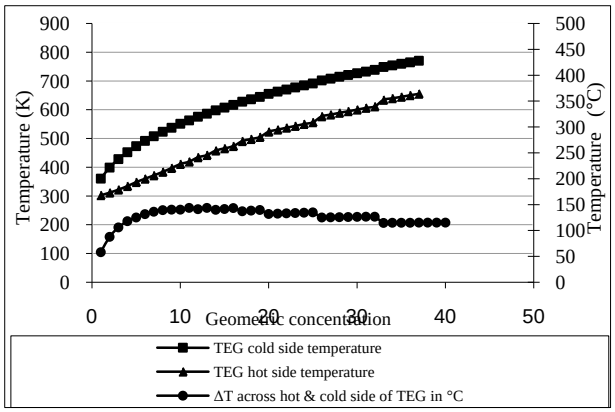

FIG. 1 GEOMETRIC CONCENTRATION VS TEG HOT & COLD SIDE TEMPERATURE AP=1 M2, I=800 W/M2, HEAT SINK FIN LENGTH=0.15M

The simulation results are as shown in Figure 10 where the temperature of the hot and cold sides of thermoelectric modules go on increasing as the geometric concentration is increased. If the target area is directly exposed to the sun without using any optical concentration device (geometric concentration=1) we can observe from the simulation results that the hot side temperature of the thermoelectric generator will reach to 360 K and the cold side temperature of the thermoelectric generator will be 302 K. The temperature difference across the hot and cold side is 58°C when the geometric concentration is 1. Further as we go on increasing the geometric concentration the temperature difference across the hot and cold side of the thermoelectric generator goes on increasing rapidly and reaches 140 °C at geometric concentration of 11 suns. The rapid increase of temperature difference will be because of increase in the heat flux concentration due to rise in geometric concentration. As we know from the laboratory tests that the thermal resistance offered by the thermoelectric generator that are considered in this simulation is 0.95°C/W. So the thermal conductivity would be approximately 1.05 W/m2K. As the heat flux concentration goes on increasing the hot side temperature will be increased rapidly, although due to very low thermal conductivity of the thermoelectric generator there will be higher temperature difference between the hot and cold side. The temperature difference remains almost constant on further increase of the geometric concentration till it reaches 15. The reason for this constant temperature is the heat sink that is attached on the bottom surface

of the thermoelectric generator (cold side of thermoelectric generator). Although the heat flux is increasing continuously at the target area and the thermal conductivity of the thermoelectric generator is assumed to be constant, the heat sink is able to dissipate the heat from the cold side of thermoelectric generator and maintain the constant temperature difference. It is also observed that any further increase in the geometric concentration will reduce the temperature difference between the hot and cold side of the thermoelectric generator. This phenomenon could be justified because we are assuming the heat sink parameters including its surface to remain constant in this simulation. It is observed that at geometric concentration of 15 we are reaching the limit of heat sink to enhance the heat transfer any further. Similar simulation was performed for increased aperture area. By increasing the aperture area we were able to increase the total amount of heat entering the system. This simulation helps us to compare the effect of change in total heat input on the hot & cold side temperatures of thermoelectric generator as well as temperature difference between hot and cold side of thermoelectric generator.

TABLE 2 INPUT PARAMETERS FOR SECOND SIMULATION

Parameters	**Value (Unit)**
Aperture Area (A_p)	1.5 m^2
Incident Solar Radiation Intensity (I)	800 W/m^2
Optical Efficiency of solar concentrator (η_{opt})	0.8
Ambient Temperature (T_a)	298 K
Thermal resistance of TEC (R_{th})	0.95 $°C/W$

Simulation results for the aperture area of 1.5 m2 and all he remaining parameters similar to the earlier simulation run are shown in Figure 11. We can observe very similar trend of temperature variation for hot and cold side of thermoelectric generator with change in geometric concentration. Initial temperature of hot and cold side of thermoelectric generator at geometric concentration of 1 will be similar to that of the earlier simulation because we have assumed to have constant solar radiation of 800W/m2 in both the cases. Even for the increased aperture area it can be observed from the simulation results that the temperature difference across the hot and cold side of thermoelectric generator goes on increasing rapidly till the geometric concentration reaches 11. Although the in this case the hot and cold side temperature id higher that in the earlier simulation with aperture area of 1m2. Similarly the value of temperature difference across the hot and cold side of thermoelectric generator is higher in this simulation due to elevated heat input to the system.

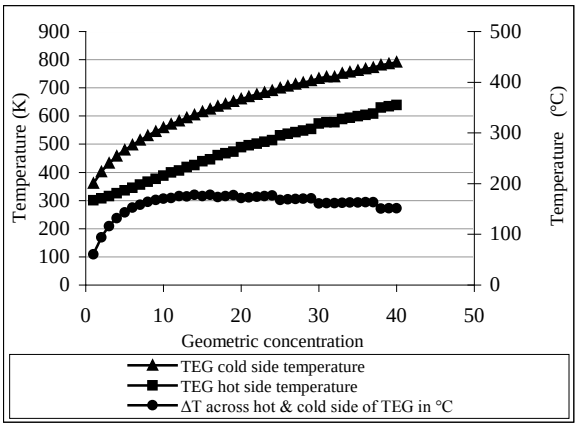

FIGURE 2 GEOMETRIC CONCENTRATION VS TEG HOT & COLD SIDE TEMPERATURE AP=1.5 M2, I=800 W/M2, HEAT SINK FIN LENGTH=0.15M

The electrical power output from the TEG for the above two configuration is predicted in the next plot.

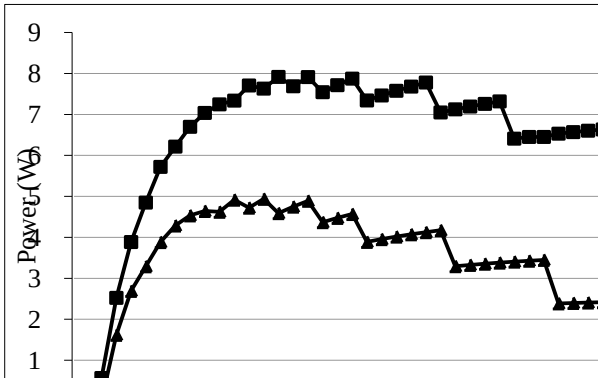

FIG. 3 TEG ELECTRIC POWER OUTPUT VS GEOMETRIC CONCENTRATION AP=1 M2, I=800 W/M2, HEAT SINK FIN LENGTH=0.15M

Predicted electrical power output from TEG versus geometric concentration curve is illustrated in figure for aperture area of 1 m2 and 1.5 m2. Electrical power output from TEG is directly proportional to the temperature difference between the hot and cold side of TEG. As the temperature difference across the hot and cold side goes on increasing the electrical power output from TEG also goes on increasing. It can be observed from Figure 12 that for the input conditions as mentioned in Table 1 and 2 the power output from

TEG would go on increasing till the geometric concentration of 11 suns. Further, power output remains steady till the geometric concentration reaches 16. But any further increase in geometric concentration will result in drop in electrical power output from the TEG. As mentioned in earlier discussion the electrical power versus geometric concentration curve supports the prediction of the optimum geometric concentration for the given input conditions. Effect of various cold side temperatures on the geometric concentration ratio was predicted in the next simulation. This simulation predicted the optimum geometric solar concentration that can by suitable to maintain different cold side temperatures of the TEG for 3 different aperture areas. Different aperture areas provided us with various heat input conditions to the system.

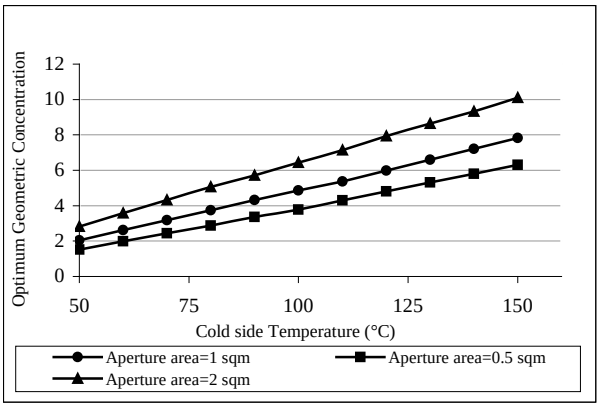

FIG. 4 OPTIMUM GEOMETRIC CONCENTRATION FOR VARIOUS COLD SIDE TEMPERATURE OF TEG AND APERTURE AREA

In Figure 14 we can observe that the computer program can predict the optimum geometric concentration for different cold side temperature of TEG and aperture are. It can be observed from the trend of the plots that as we allow the cold side temperature to rise we can have higher geometric concentration can be used. This behavior of the geometric concentration as we allow the cold side temperature to reach higher value is obvious because by increasing the allowable cold side temperature of TEG we are reducing the load on the heat sink to dissipate the heat. Similar trend is observed in case of increase in aperture area. It is predicted that we can reach higher geometric concentration as we go on increasing aperture area. With increase in aperture area we can have larger target area for same geometric concentration. Larger target area results in increased number of possible fins on the heat sink, eventually increasing the estimated optimum geometric concentration.

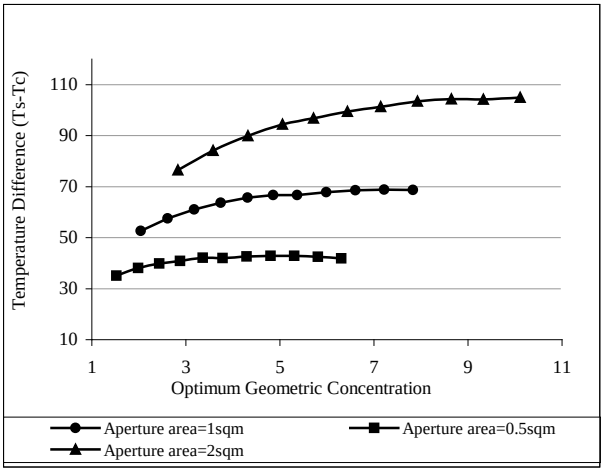

FIG. 5 TEMPERATURE DIFFERENCE ACROSS HOT AND COLD SIDE OF TEG FOR DIFFERENT OPTIMUM GEOMETRIC CONCENTRATIONS AND APERTURE AREAS

Figure 15 illustrates the temperature difference achieved across the hot and cold side of TEG during the previous simulation for different aperture areas. For all three aperture areas it was observed that the temperature difference across hot and cold side of TEG will go on reducing and eventually stagnate as we allow cold side to reach higher temperatures. If we increase the aperture area we could achieve higher temperature difference across hot and cold side of TEG. We can achieve higher temperature difference with increased aperture area due to the larger target areas available eventually increasing the number of fins on the heat sink that are responsible for enhancing the heat transfer rate from the cold side of TEG.

Conclusions

The theoretical analysis and the computer model successfully demonstrated that we can predict the optimum geometric solar concentration for different input conditions. From the results of first and second simulation with aperture area 1m2 and 2m2 respectively we can conclude that optimum geometric solar concentration for certain heat sink configuration remains constant even if we change the aperture area (heat input to the system). In this case the optimum geometric solar concentration is determined depending on the trend of the temperature difference between the cold and the hot side of the TEG. Certainly the electrical power output plots follow the same trend as that of the temperature difference between the hot and cold side of TEG. As we go on increasing the allowable cold side temperature for TEG, the optimum geometric will go on increasing.

Increase in aperture area will also show us the similar trend. It can also be concluded that we can achieve higher temperature difference between the hot and cold side if we increase the aperture area in turn increasing the electrical power output from TEG. Theoretical analysis and the energy balance equations developed in this paper can be useful to optimize the design of the concentrated solar thermal system with thermoelectric generator as a power generation device. This thermal analysis could also be used to optimize the design for other solar thermal applications with little modification.

REFERENCES

3M (2009). "Factors Influencing the Optical Efficiency of Fresnel Lens Concentrators."

Al-Jumaily, K. E. J. and M. K. A. Al-Kaysi (1998). "The study of the performance and efficiency of flat linear Fresnel lens collector with sun tracking system in Iraq." Renewable Energy **14**(1-4): 41-48.

Fujii, T. and H. Imura (1972). "Natural-convection heat transfer from a plate with arbitrary inclination." International Journal of Heat and Mass Transfer **15**(4): 755-764, IN755-IN756, 765-767.

Holman, J. P. (1990). Heat Transfer. New York, McGraw-Hill Publishing Company.

Lloyd, J. R. and W. R. Moran (1974). "Natural Convection Adjacent to Horizontal Surface of Various Planforms." Journal of Heat Transfer **96**(4): 443-447.

Zhang, X. and D. Liu (2010). "Optimum geometric arrangement of vertical rectangular fin arrays in natural convection." Energy Conversion and Management **51**(12): 2449-2456.